Temperature distributions in concrete bridges for Indian summer conditions-1

D. S. Prakash Rao

Despite the growing awareness of the importance of temperature-induced stresses in concrete bridges, no systematic study is yet available for the Indian summer conditions with high ambient temperatuces. The first part of the paper, presented here, studies the influence of various parameters, such as the night-sky conditions, blacktop thickness, wind velocity and cross-section of the bridge. The second part of the paper, to be published later, will deal with critical temperature distributions in concrete bridges for Indian summer conditions, based on series solution which satisfies the boundary conditions and the governing differential equation exactly.

Temperature-induced stresses in concrete bridges are not always considered in design despite the awareness of their deleterious effects on structures, particularly prestressed concrete structures[1-6]. This is because of the absence of suitable provisions in the codes of practice and lack of data on these aspects. The variation of temperatures through the depth of a concrete structure, and of the accompanying stresses, are functions of several parameters, environmental as well as structural; while the temperature distribution depends upon the ambient conditions, thermal properties of concrete and the cross-section, the stresses depend upon the cross-section, support conditions and the elastic and thermal properties of concrete[1-4]. The physical properties of the material have more or less well-established values but the ambient conditions vary from place to place. The distributions of temperature in concrete bridges are presented in this paper for various possible cross-sections of elements for the Indian summer conditions, with high ambient conditions.

The meteorological data of New Delhi were taken for the analysis as the representative conditions. The temperature distributions in various elements of a bridge superstructure, such as slabs, webs and the slabs above and below the air cell in a box girder, were obtained by linear heat-flow analysis, using a series solution. The results obtained were compared with the solution given by the Finite Difference Method (FDM)[7]. It was found that the maximum soffit tensile stresses in a continuous bridge occur for the cold-top condition (top surface cooler than the interior), rather than the hot-top condition for the meteorological data assumed, Figure 1. Design temperature distributions are proposed, based on the analysis presented and the influence of the parameters, such as the wind velocity, blacktop thickness and girder depth are studied. The soffit tensile stresses in two-span and multi-span continuous bridges under the computed and proposed temperature distributions are compared to check the validity of the proposed distributions. The proposed temperature distributions will be valid for the climatic conditions similar to the assumed data.

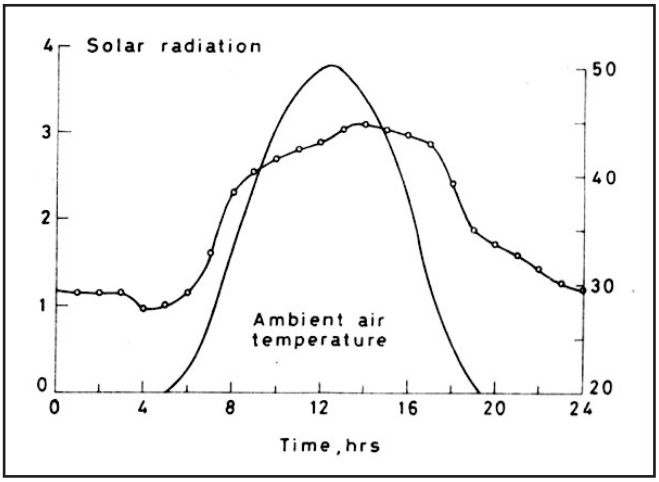

Figure 1. Hourly variation of solar radiation and ambient air temperature on a harsh summer day at New Delhi (May 16, 1981)

Ambient conditions and data

The most important step in a thermal-stress analysis is the proper choice of meteorological data. The published data are not always in a form suitable for direct use and often only the minimum, mean and maximum values of the solar radiation and mean values of temperatures and wind velocity are valuable[8]. However, a study of these data brings out several features typical to an Indian summer — a fairly high amount of solar radiation, high ambient temperatures and low mean wind velocities[2-8]. Such conditions persist continuously for several days and the peak values of temperature and solar radiation are reached in the month of May in most parts of the country[2-8]. In view of these factors, the data of May 16, 1981, recorded in New Delhi, can be taken as one of the worst possible combinations, Figure 1[9].

The amount of heat transferred at the boundary of air and the bridge surface depends upon the absorptivity coefficient, α, and the heat transfer coefficient, h_1, for these two media. The absorptivity coefficient is a function of the surface colour and texture, and varies from α =0.9 for a black surface to about 0.5 for a fresh concrete surface[1, 3, 10]. For the analysis presented α=0.9 was assumed, unless mentioned otherwise. The heat-transfer coefficient is usually assumed to be a linear function of the wind velocity, including the convective and radiative heat losses[1].

$h_1 = 13.5 + 3.88v$... (1)

$h_2 = h_1/2$ ... (2)

where, h_1 = heat-transfer coefficient in J/m²/°K/s for the top surface

h_2 = heat-transfer coefficient for the bottom surface

v = wind velocity in m/s.

The mean wind velocity for New Delhi in the month of May is about 3.3m/s, but a wind speed of less than 2.Om/s is likely to persist on summer afternoons and still wind conditions are also not uncommon[2, 8]. Further, in surroundings where the surface wind velocities are likely to get reduced, a reduction factor of 0.7 is recommended on the mean wind velocity[1]. Based on these data as well as the parametric studies presented later, a mean wind velocity of 1.5m/s was assumed.

The radiation losses from the surface are increased by clear and cloudless night conditions, which lower the temperatures at the top surface. These losses were computed as per the Stefan-Boltzmann's law[10]. The emissivity coefficient, ε, for clear sky was taken as 0.9 and as zero for clouded sky condition. In India, the summer nights are usually clear and cloudless; an emissivity coefficient ε = 0.9 was thus assumed in the analysis unless mentioned otherwise.

Heat-flow analysis

The linear heat-flow equation and the governing boundary conditions for a multi-layered medium are fairly well known, and are thus not dealt with here in any detail[1-4, 7, 11]. However, it may be mentioned that a series solution is assumed for the temperature distribution in a layer n of the multi-layered system, shown in Figure 2, in the form:

$$T_n = A_{on}x + B_{on} + \sum_{m=1}^{00}\left(A_{mn}{}_2{}^{\beta_{mn}x} + B_{mn}{}_2{}^{-\beta_{mn}x}\right)e^{im\omega t} \quad \text{... (3)}$$

where,

A_{on}, B_{on}, A_{mn} and B_{mn} are the constants pertaining to the n^{th} layer

ω = 2/24

$$\beta_{mn} = \sqrt{(im\omega\rho_n c_n/k_n)}$$

p_{mn} = density of n^{th} layer

c_n = specific heat of n^{th} layer

k_n = conductivity of n_{th} layer

m = number of term

$$i = \sqrt{-1}$$

This distribution satisfies the governing differential equation by virtue of the exponential functions chosen,

$$k_n = \frac{a^2r}{ax^2} = \rho_n c_n \frac{ar}{ar}$$

The constants of equation (3) are evaluated by solving the simultaneous equations obtained from the boundary conditions at the top and bottom surfaces and at the interfaces of the medium[1-4, 7, 11]. These series converge rapidly and usually six terms of the series are adequate for the convergence of the stresses to 1 percent accuracy.

Comparison with FDM

The temperature distribution obtained by the series (equation 3) was compared with that obtained by the FDM for several cases of slabs, beams and box girders[7]. The computer program developed by Priestley was used for this comparison[7]. The

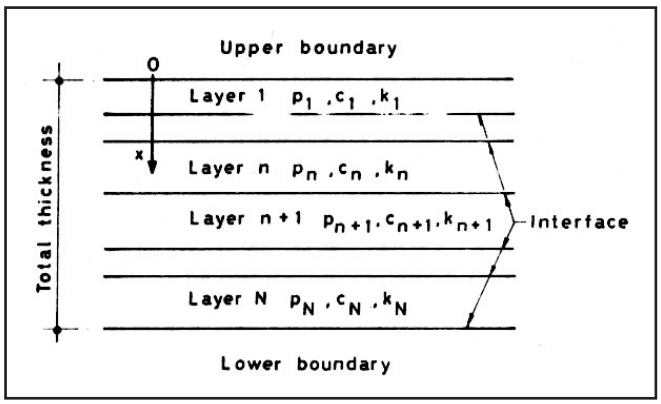

Figure 2. Multi-layered system for heat-flow analysis

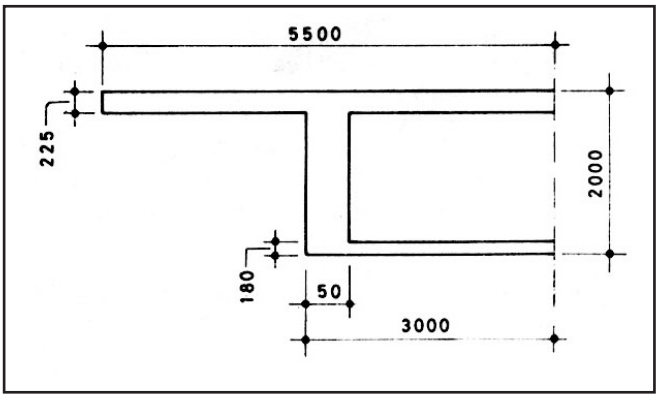

Figure 3. Cross-section of a prestressed concrete box girder

Table 1. Material properties assumed

Material property		Material: Concrete	Material: Bitumen	Air
Conductivity, J/m/s/°K	k	1.384	0.744	0.225
Specific heat, J/kg/°K	c	922.0	838.0	922.0
Density, kg/m^3	ρ	248.0	2240.0	1.3
Modulus of elasticity, GN/m^2	E	35.0	0.1	0.0
Coefficient of thermal expansion X 10^6, M/M/°K	α	10.8	20.0	0.0

solution obtained by the FDM depends upon the space and time intervals, the assumed initial temperature distribution and the number of iterations performed. Most of the investigators assumed a uniform temperature distribution for the initial nodal values, equal to the ambient temperature at dawn, and one or two iterations were performed for the same meteorological data. The temperature distribution that caused the maximum soffit tensile stresses at the end of these limited numbers of iterations was taken as critical for design purposes. Such an approach, while satisfactory for thin slabs, is likely in general to lead to an incorrect temperature distribution that does not satisfy the governing differential equation and the boundary conditions. Further, the temperature distribution in the structure after only one or two iterations depends to a large extent on the initial temperatures chosen. It is also well-known that the temperature distribution in the structure is non-linear even at dawn and that its average temperature at dawn is about the same as the mean ambient temperature of the

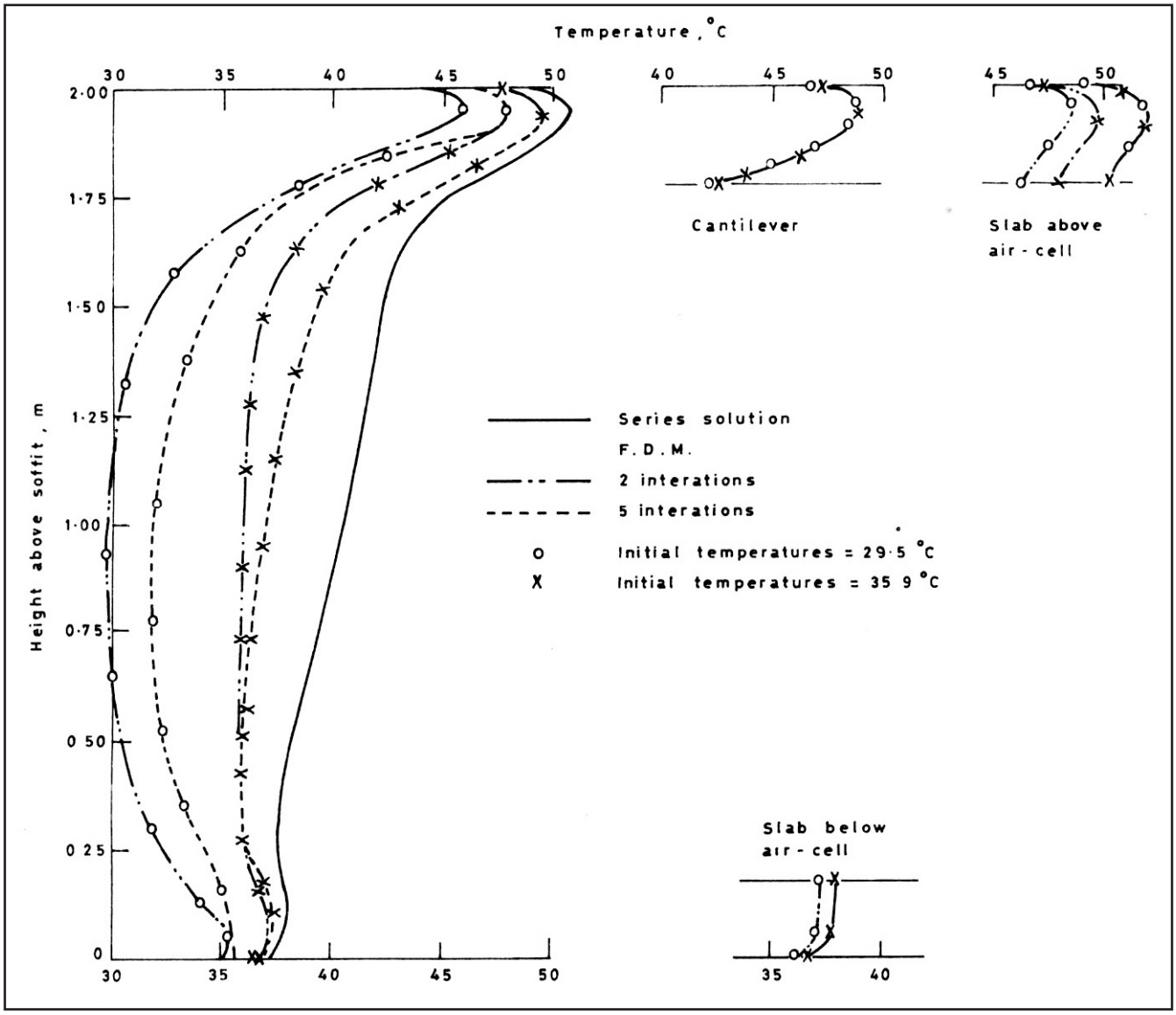

Figure 4. Temperature distribution at 2100 hours in the box girder based on FDM and series solution (clear night sky, e = 0.9, a = 0.9 and blacktop thickness t_b = 50mm)

preceding day[3, 12]. Thus, when using the FDM, it will not be correct to terminate the iterations without obtaining convergence.

For the sake of illustration, the box girder shown in Figure 3 was analysed for heat flow for the data of New Delhi, Figure 1, by using the series solution as well as the FDM, Figure 4. The material properties assumed in this article are given in Table 1[1]. The solution of the FDM was iterated several times and the temperature distribution was compared with that of the series solution for each iteration. A blacktop thickness, t_b, of 50mm, absorptivity coefficient α=0.9, emissivity coefficient ε=0.9 (clear night sky) and a wind velocity of 1.5m/s were assumed. For the FDM, two different uniform initial temperatures of 29.5°C (the ambient temperature at the start of the iterations) and 35.9° (the mean ambient temperature of the day) were assumed as the starting values. The box girder was treated as comprising three different paths for heat flow, the cantilever slab of 225-mm thickness, the 2.0-m deep web and the top and bottom slabs enclosing the air cell, Figure 3. The temperature distributions at 2100 hours, after 2,5 and 20 iterations, are shown in Figure 4, since the maximum soffit tensile stresses occur at 2100 hours for these data.

It can be seen, for the cantilever slab, that the temperature distributions given by the series solution and the FDM coincide after just 2 iterations, while five iterations are needed for the air cell case for both the initial temperatures assumed. The series solution and the FDM show good agreement for the web only after about 20 iterations. Further, it can be seen that the temperature distributions in the web after 2 iterations vary considerably for the two initial temperatures assumed.

This process was repeated for several dimensions of slabs and web and it was found that the solution of FDM converges to that of the series in every case; the number of iterations varying from 2 for a 200-mm thick slab to about 80 for a 4.0-m deep web. For further studies, the temperature distribution given by the proposed series solution (equation 3) was used.

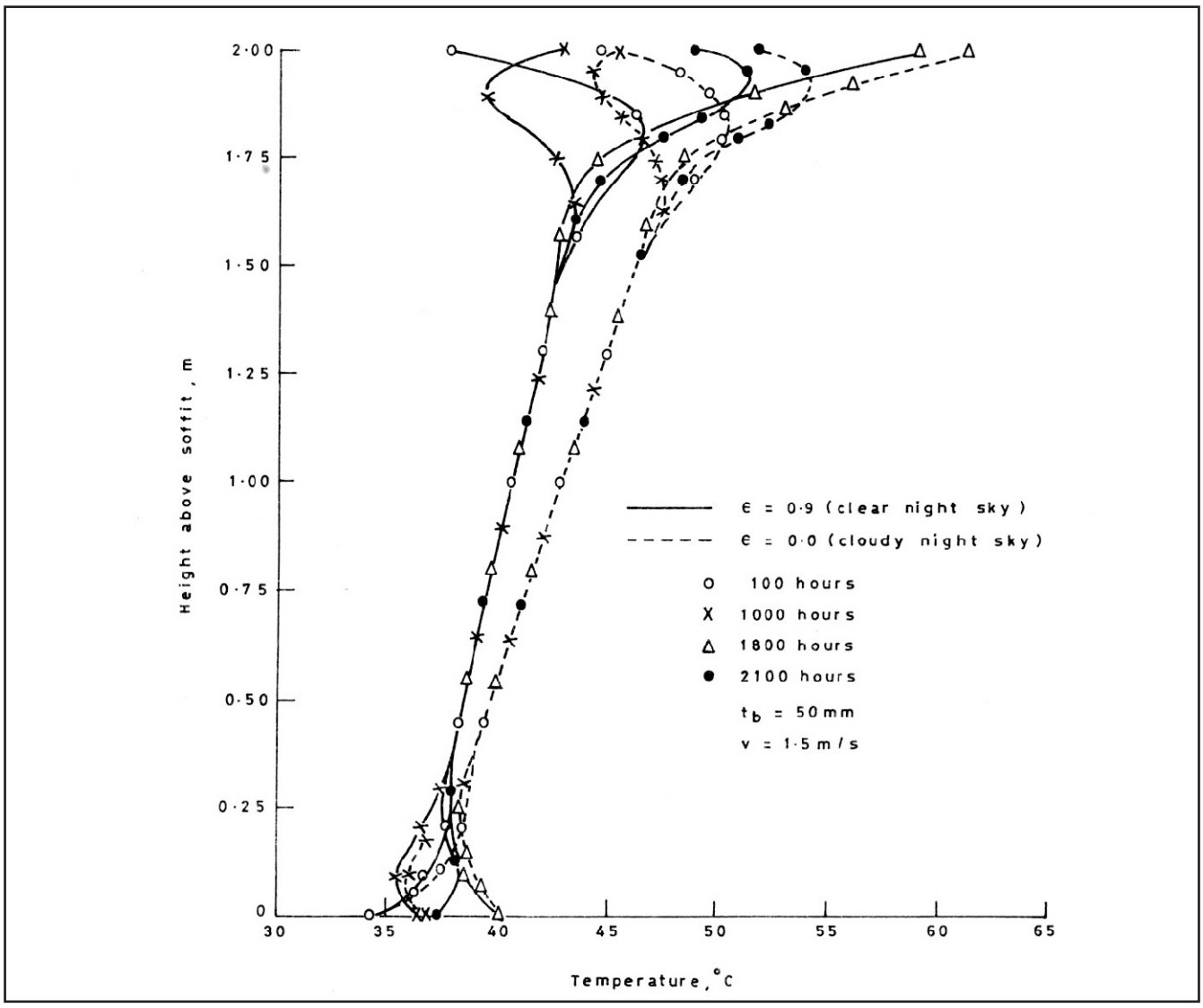

Figure 5. Temperature distributions along the web of the box girder at various times of the day

Stress analysis

The temperature distribution so obtained at hourly intervals was analysed for computing the longitudinal stresses in the structure. The analysis was based on the general procedure outlined by Priestley[1]. The bridge was assumed to be of prismatic section with full restraint against flexure at the supports, representing an intermediate span of a continuous bridge of several equal spans. The temperature distribution in various parts of the cross-section, such as the cantilever slab, web and the slabs above and below the air cell in a box girder, was taken into account. The soffit tensile stresses were computed at hourly intervals and the temperature distribution corresponding to the maximum soffit tensile stress was noted for each case. Several cases of slabs, T-beams and box girders were analysed for this purpose. The temperature distributions so obtained were simplified in order to obtain a set of linear or bi-linear distributions suitable for temperature stress analysis without recourse to a detailed heat flow analysis.

These simplified distributions for various types of cross-sectional elements were further utilised in a complete analysis of bridges based on the Finite Strip Method (FSM)[13]. The thermal loading caused by the temperature distributions was treated as equivalent in-plane and bending forces by using the strain energy method[14]. The longitudinal stresses and transverse moments obtained by the FSM and by the approximate analysis were compared for several cases.

Response of the bridge

The temperature distrubutions down the depth of the web of the box girder section, Figure 3, are plotted in Figure 5 for various times of the day. The temperatures were computed for both cloudy and clear night-sky conditions with t_b = 50mm. It can be seen that, during a single day, the temperature variation is caused only within about 500mm of the top and bottom surfaces of the web and the temperatures remain unaffected in the interior zone. The thinner the section the smaller is the

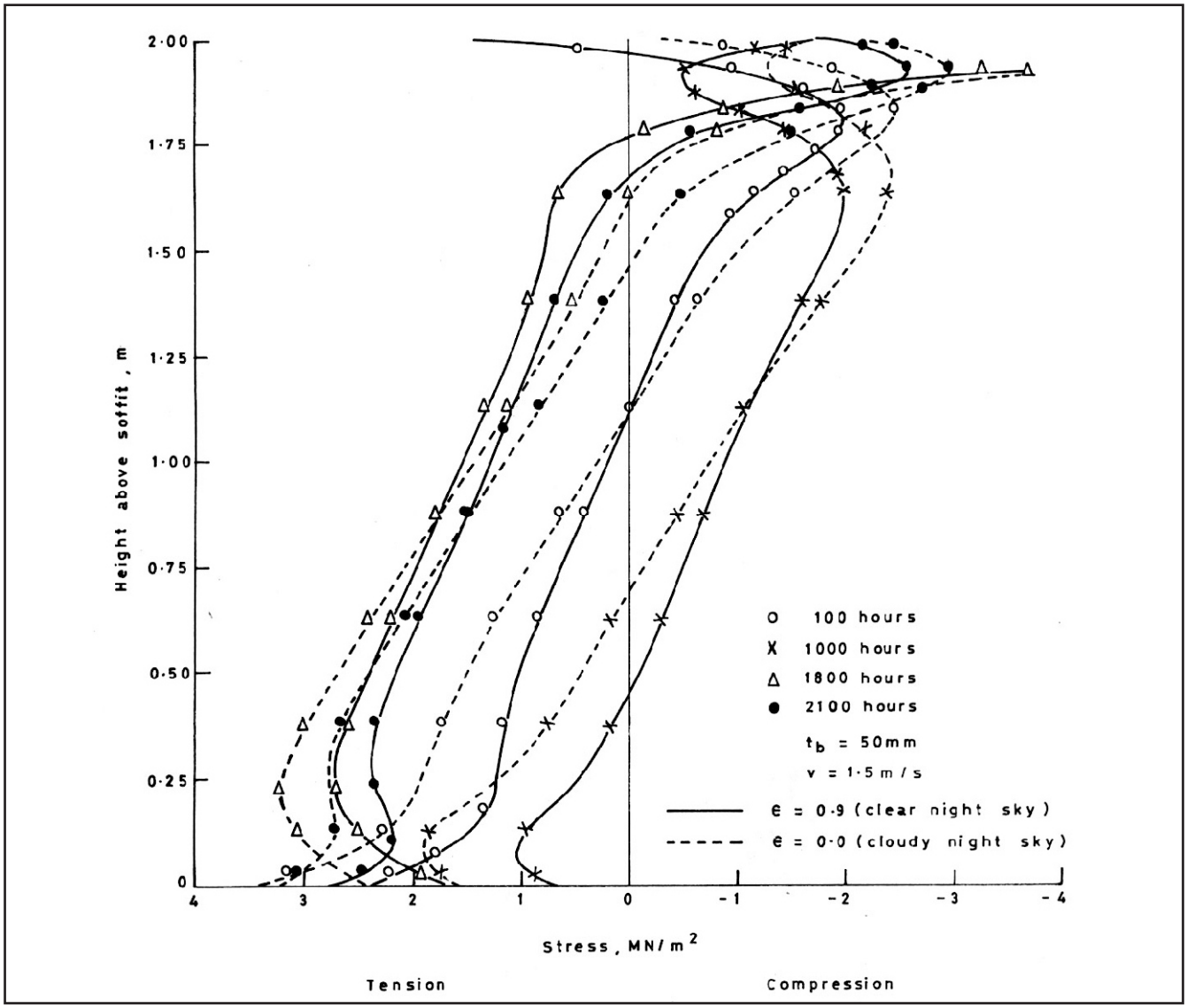

Figure 6. Stress distributions along the web of the box girder corresponding to the temperature distributions shown in Figure 5

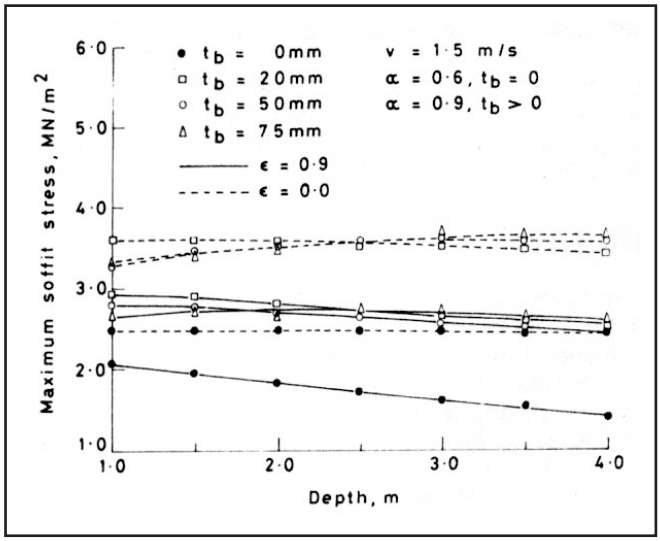

Figure 7. Variation of the maximum soffit tensile stress for the web of the box girder for various depths and blacktop thicknesses

thermal inertia and, thus, the quicker is the response to the changes in ambient conditions. It can be presumed that the temperatures in the interior zone depend upon the ambient conditions prevailing over several preceding days and build up as the summer advances, attaining a definite profile during the peak summer period.

The stress distributions in the continuous box girder corresponding to these temperature distributions, Figure 5, are plotted in Figure 6. It can be seen that for both clear night and cloudy night conditions, it is the cold-top condition of the structure that induces the highest soffit tensile stresses, rather than the hot-top condition. In the case of clear night condition, the maximum soffit tension occurs at 2100 hours and for the cloudy night condition at 0100 hours. During the afternoon, when the top surface is the hottest, the bottom surface also gets heated up thereby reducing the tensile stresses considerably. Later in the evening, the soffit will be cooler than the interior and this condition increases the soffit tensile stress. In all the cases analysed it was noticed that the maximum soffit tension occurs between 2000 to 2200 hours for ε = 0.9 and between 2400

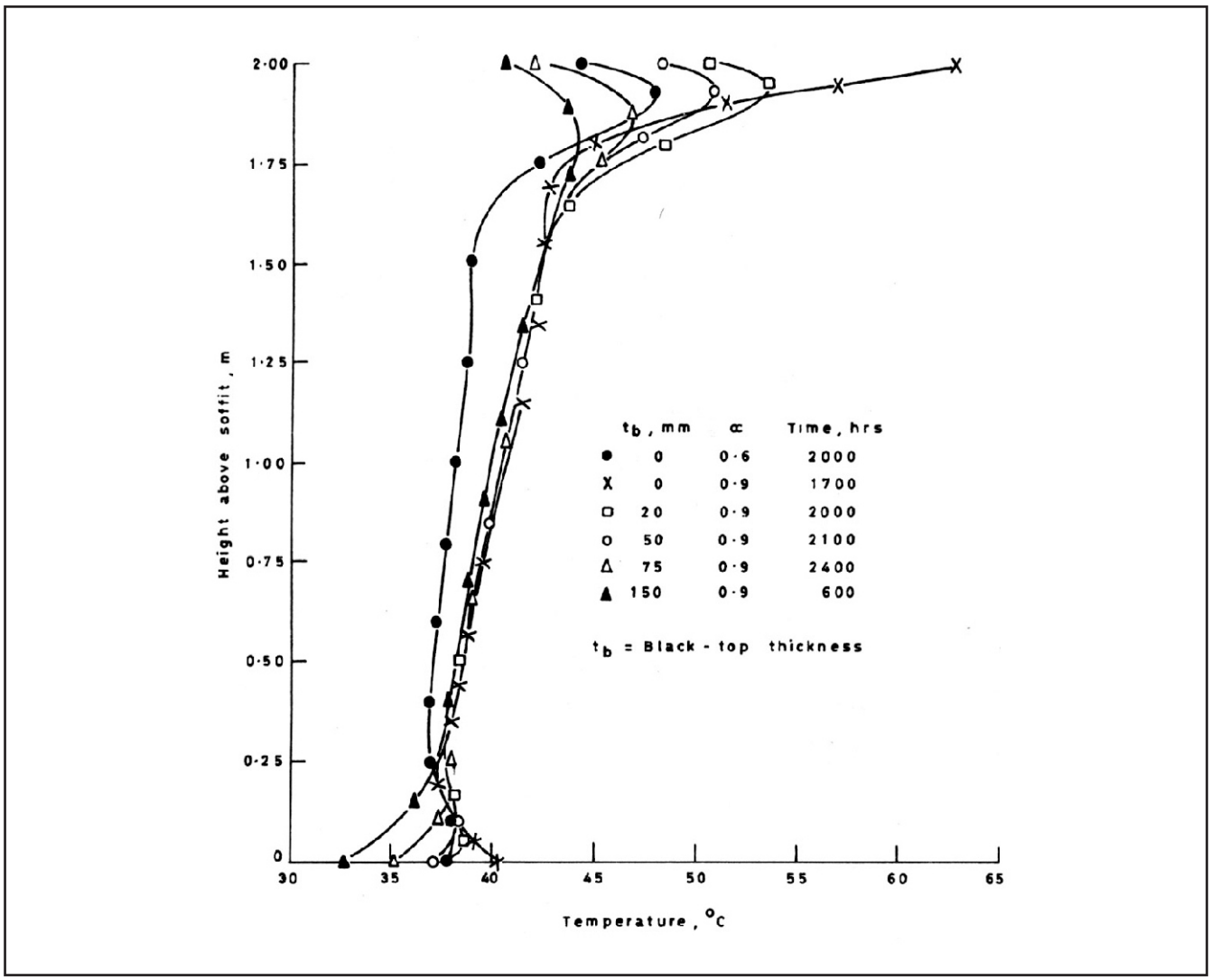

Figure 8. Distributions of temperatures through the web of the box girder corresponding to the maximum soffit tensile stress for various blacktop thicknesses

to 0400 hours for e = 0.0. Since the clear night-sky conditions are relevant for the Indian summer, the temperature distribution at 2100 hours was adopted for further analysis. It must be mentioned here that the curvature of the beam and, consequently, the upward displacement at the midspan and the support restraining moment are the highest around 1600 hours. However, the soffit tension at that time will be lower than that at 2100 hours on account of the soffit temperature being high. The soffit gets cooled faster than the top surface in the evening hours, and this increases the soffit tension even though the restraining moments are lower. The soffit tension is reduced later on as the top layers also get cooled. The cycle is repeated the following day as the solar radiation commences.

Influence of night-sky conditions

As mentioned already, a clear night increases the radiative losses from the top surface, thereby decreasing the top-surface

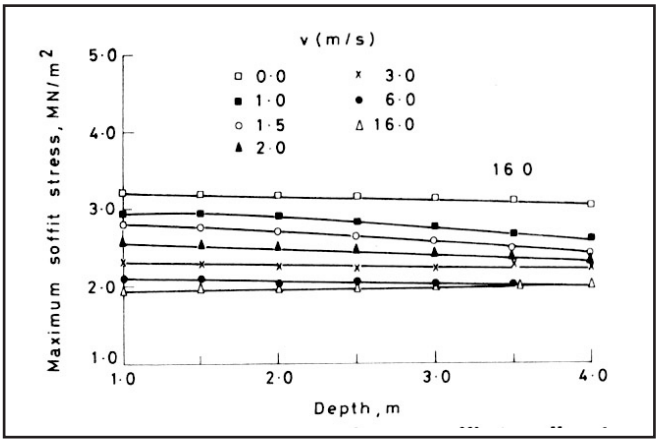

Figure 10. Variation of the maximum soffit tensile stress at the web of the box girder for various depths and wind velocities

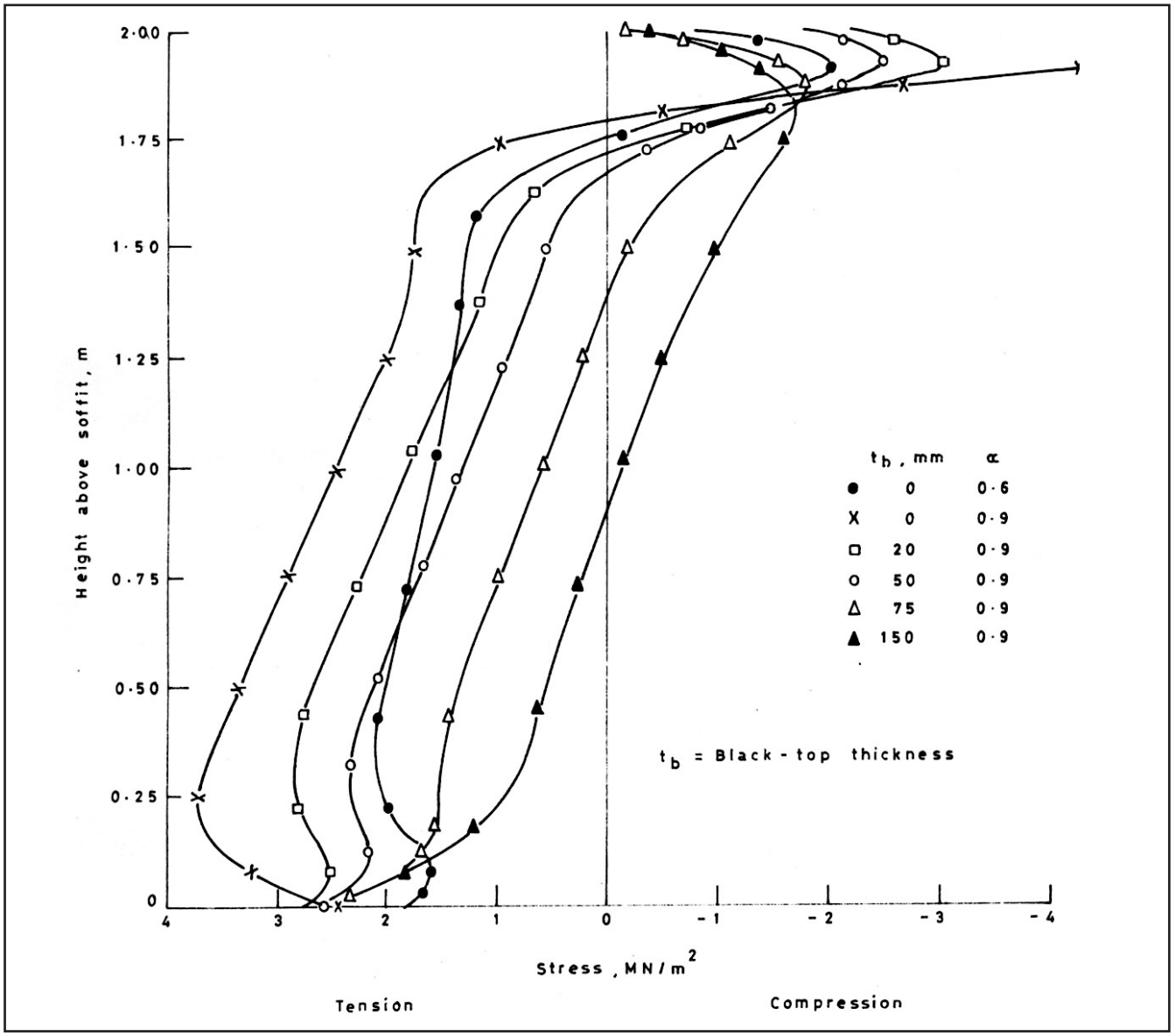

Figure 9. Stress distributions along the web of the box girder corresponding to the maximum soffit tensile stress for various blacktop thicknesses

temperatures. This is reflected in the soffit tensile stress, which is lower for clear night condition than for the cloudy night sky, Figure 6. This was found to be valid for various types of bridges. The variation of the maximum soffit tensile stress for various depths of the box girder and blacktop thickness is plotted in Figure 7. In general, the stresses are lower for clear night sky, differing up to about 40 percent from those for the cloudy night-sky condition. This extreme difference occurs for the case of t_b = 0mm and a girder depth of 4.0m. However, for other cases the difference was about 20 to 30 percent.

Nevertheless, a clear night condition, E = 0.9, was assumed in the analysis for developing the design temperature distributions, since this is relevant to the Indian conditions.

Influence of blacktop thickness

It is generally believed that blacktopping reduces heat flow into the bridge surface and the thermal gradients and resulting soffit tensile stresses are, likewise, smaller[1,3,4,7]. The variation of maximum soffit tensile stress for the web of the box girder for various thicknesses of blacktopping is shown in Figure 7. The blacktop thickness was varied from Omm to 75mm, the absorptivity coefficient a being taken as 0.6 for the concrete surface (zero blacktop thickness) instead of the usual value of 0.9. The maximum soffit tension occurred invariably for the cold-top condition for all the blacktop thicknesses. The variation in the maximum soffit tensile stress, as the blacktop thickness was varied from 20mm to 75mm, was barely 10 percent when the depth of the girder was in the range of 1.0m to 4.0m. This difference was still smaller for the cloudy night-sky condition.

In the absence of blacktopping, the absorptivity of the top surface is reduced considerably, the value of a for fresh concrete being 0.5 to 0.7 [1.3.10]. The same box girder, analysed for a = 0.9 and no blacktopping, experienced the maximum soffit tension at 1700 hours, whereas for a = 0.6 the maximum tension occurred at 2000 hours under the cold-top condition, Figures 8 and 9. The temperature distributions that induce maximum soffit tension in a 2.0-m deep box girder for various blacktop thicknesses are plotted in Figure 8. It can be said in general that blacktopping acts as an insulator and reduces top-surface temperatures during the day but does not allow the top surface to cool in the evening hours. As a consequence, the temperature difference between the top and bottom regions of the girder is about the same for both thick as well as relatively thin blacktoppings. Thus, for the ambient conditions assumed in this article, the difference in the soffit tensile stresses for various blacktop thicknesses is not significant. For further analysis a blacktop thickness of 50mm was assumed.

Influence of wind velocity

The convective heat losses are proportional to wind velocity, the tendency of the wind being to reduce the amount of heat flow into the concrete surface and to bring the surface temperatures close to the ambient temperature[1,7,10]. The influence of wind velocity on the soffit tensile stresses was studied by varying the wind velocity from 0m/s to 16.0m/s; the corresponding heat-transfer coefficients were computed by the equations (1) and (2). The results of the analysis are plotted in Figure 10 for various depths of the box girder. The soffit tension decreases significantly at first as the wind velocity is increased from Om/s, but after about v = 12.0m/s there is little change in the soffit tension. The reduction in soffit tension is about 34 percent for a 1.0-m deep box girder when the wind velocity is increased from Om/s to 6.0m/s. The corresponding difference between the soffit tensile stresses for the wind speeds of 1.0m/s and 2.Om/s is barely 10 percent, Figure 10.

(to be Continued)

References

1. PRIESTLEY, M. J. N. and BUCKLE, I. G. Ambient thermal response of concrete bridges. RRU Bulletin 42, National Roads Board, New Zealand, 1979. p. 83.
2. BHASIN, P.C. and CHAKRABARTI, S. P. Temperature difference stresses in fully prestressed concrete bridge decks. The Bridge and Structural Engineer, September 1982 and December 1982.
3. EMERSON, M. The calculation of the distribution of temperature in bridges. TRRL Report LR 561, Department of the Environment, 1973. p. 33.
4. WHITE, I.G. Non-linear differential temperature distributions in concrete structures: a review of the current literature. Technical Report 525, Cement and Concrete Association, 1979. p. 23.
5. PRAKASH RAO, D. S. and co-authors. Literature survey on in-situ testing of concrete bridges. Materials and Structures, RILEM, No. 96, November and December 1982. pp. 457-466.
6. PRAKASH RAO, D. S. and co-authors. In-situ testing of bridge superstructure-a state of the art report. Research Report, Structural Engineering Research Centre, Roorkee, India, 1983.
7. PRIESTEY, M. J. N. Linear heat flow and thermal stress analysis of concrete bridge decks. Research Report. University of Canterbury, 1976. p. 24.
8. MANI, A. Handbook of solar radiation data for India 1980. Allied Publishers, New Delhi, 1981. p. 498.
9. SUBHASH CHANDRA. Solar thermal modelling of buildings and space conditioning systems. Ph.D. Thesis, Indian Institute of Technology, Delhi, March 1982.
10. THRELKELD, J. L. Thermal environmental engineering. Englewood Cliffs, New Jersey, Prentice Hall, 1970.
11. PRAKASH RAO, D. S. Temperature distributions and stresses in concrete bridges. ACI Journal, July-August 1986.
12. CHURCHWARD, A. J. and SOKAL, V. J. Prediction of temperatures in concrete bridges. Journal of the Structural Division, Proceedings of the American Society of Civil Engineers, Vol. 107, No. ST 11, November 1981. pp. 2163-2176.
13. CHEUNG, Y. K. Finite strip method in structural analysis. Pergamon Press, Oxford, 1976. p. 232.
14. WILSON, E. L. Structural analysis of axisymmetric solids. American Institute of Aeronautics and Astronautics Journal, Vol. 3, 1965. pp. 2269-2274.

D. S. Prakash Rao, Department of Civil Engineering, University of Melbourne, Australia.

(Source: ICJ August 1987, Vol. 61, No. 8, pp. 211-218)